J Mater Sci (2010) 45:5370–5377
DOI 10.1007/s10853-010-4586-1

Hydrolytic stability of sodium silicate gels in the presence of aluminum

I. Giannopoulou · D. Panias

Received: 25 November 2009 / Accepted: 30 April 2010 / Published online: 11 May 2010

Abstract Polycondensation in alkali silicate solutions comprises a fundamental process of the geopolymerization technology. Previous works had shown that the hydrolytic stability of sodium silicate gels depends on the SiO_2/Na_2O ratio. Sodium silicate gels totally insoluble in water can be produced at SiO_2/Na_2O molar ratios higher than 4.4. This article aims at elucidating the effect of tetra-coordinated aluminum addition on the hydrolytic stability of sodium silicate gels. According to the results, the aluminum addition stabilizes the sodium silicate gels in an aqueous environment. A sodium silicate gel with SiO_2/Na_2O molar ratio 3.48, which is totally soluble in deionized water at ambient temperature, can be transformed to insoluble sodium hydroaluminosilicates with the addition of tetrahedral aluminum at Al/Si molar ratios higher than 0.08. In addition, this article studies the structure of prepared sodium hydroaluminosilicates and draws very useful conclusions for the geopolymerization technology.

Introduction

The alkali silicate gels comprise the matrix of a new family of inorganic polymeric materials called "geopolymers" [1–4]. The geopolymerization technology is a low cost, green technology [5] that can transform a variety of solid amorphous silicate and aluminosilicate raw materials [6–10] to useful products with high added value [6–8, 10–13]. Previous study [2] has shown that the hydrolytic stability of sodium silicate gels depends on the SiO_2/Na_2O ratio. Generally speaking, the higher the ratio, the higher the hydrolytic stability is. Sodium silicate gels with molar ratio higher than 4.4 are characterized as practically insoluble in water. Moreover, preliminary tests [2] have shown that the addition of aluminum in sodium silicate gels can substantially improve their hydrolytic stability. Therefore, this study attempts to elucidate the role of the incorporated aluminum on the structure and the hydrolytic stability of the sodium hydroaluminosilicates.

I. Giannopoulou · D. Panias (✉)
Laboratory of Metallurgy, School of Mining and Metallurgical Engineering, National Technical University of Athens, 15780 Zografou, Athens, Greece
e-mail: panias@metal.ntua.gr

Materials and methods

The sodium hydroaluminosilicates were prepared by mixing appropriate amounts of a sodium silicate solution, a sodium aluminate solution, and silica fumes. The standard sodium silicate solution was a commercial water–glass solution with SiO_2/Na_2O molar ratio 3.48 and density 1346 kg/m^3 supplied by Merck. The sodium aluminate solution was prepared according to the following procedure: 13 g of pure hydrargillite ($Al_2O_3 \cdot 3H_2O$) and 11.5 g of sodium hydroxide commercially available by Merck were added into an Inconel autoclave that contained 160 mL of distilled water. The pulp was heated at 160 °C for 1 h and the solids were totally dissolved. After rapid cooling, the liquor was diluted to a final volume of 200 mL containing 44.5-g/L Na_2O and 42.5-g/L Al_2O_3. Silicon (IV) oxide amorphous fumes (purity 99.8% and surface area 300–350 m^2/g) supplied by Alfa Aesar were used to prepare sodium hydroaluminosilicates with a pre-fixed SiO_2/Na_2O ratio. The prepared sodium hydroaluminosilicates had a fixed SiO_2/Na_2O molar ratio 3.48, while their Al/Si molar ratio was varied in the region 0–0.33 (Table 1).

Table 1 Composition of sodium hydroaluminosilicates (SiO_2/Na_2O molar ratio 3.48)

Al/Si molar ratio	0	0.02	0.04	0.08	0.17	0.33
Waterglass (mL)	100	86.63	75.21	55.38	29.29	0
Sodium aluminate solution (mL)	0	13.37	24.79	44.62	70.74	100
Silica fumes (g)	0	1.94	3.66	6.65	10.59	14.99

The hydroaluminosilicates were prepared by accelerated polycondensation in sodium aluminosilicate solutions. Accelerated polycondensation was performed in an electrical oven equipped with a diaphragm vacuum pump at 60 °C by gradual evaporation of water. The vacuum oven was operated on daily cycles. Each cycle consisted of 2 h evaporation under vacuum followed by 1 h evaporation at atmospheric pressure repeated thrice and then 15 h evaporation at atmospheric pressure. The whole duration of each polycondensation experiment comprised five daily cycles during which 80–85% of the initially contained water was evaporated.

The structure of the prepared hydroaluminosilicates was determined by means of X-ray diffractometry (XRD) utilizing a Siemens D5000 diffractometer (Cu Kα radiation, 40 kV, 30 mA, 2°/min), FTIR utilizing a Perking Elmer 880 spectrometer (KBr pellets, sample/KBr = 1:200), thermal analysis (TG/DTA) utilizing a Setaram Labsys analyzer (Helium atmosphere, 5 °C/min), and SEM utilizing a Jeol JSM-type SEM. Scanning electron microscopy was performed on as-prepared as well as fractured surfaces.

The hydrolytic stability of the prepared sodium hydroaluminosilicates was determined through a dissolution test in deionized water. An aliquot of 2 g of hydroaluminosilicate was totally immersed in 100 mL of deionized water and let in contact for 24 h at ambient temperature. Then, the solution was filtrated and analyzed for its silicon and its aluminum content by inductively coupled plasma mass spectrometer.

Results and discussion

The effect of aluminum incorporation on the hydrolytic stability of the sodium silicate gels with SiO_2/Na_2O molar ratio 3.48 is shown in Fig. 1. The sodium silicate gel with SiO_2/Na_2O molar ratio 3.48 was totally dissolved in deionized water at ambient temperature as is seen in Fig. 1. The hydrolytic stability of the hydroaluminosilicates was significantly improved as the Al/Si ratio increased and they were practically insoluble in deionized water for Al/Si molar ratios higher than 0.08.

It is noteworthy that the aluminum solubility was always substantially lower than the silicon one as is clearly seen in Fig. 1. This observation was an indication that the sodium

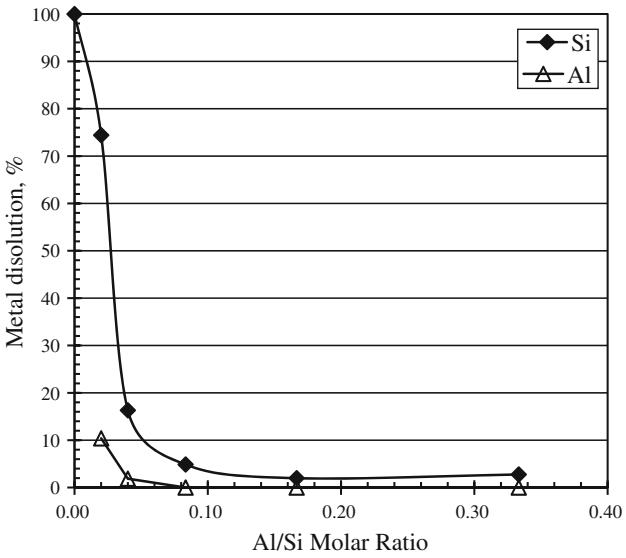

Fig. 1 Hydrolytic stability of sodium hydroaluminosilicates with fixed SiO_2/Na_2O molar ratio 3.48 as a function of Al/Si ratio

hydroaluminosilicates were not homogeneous in composition. Their XRD analysis shown in Fig. 2 was not able to detect different phases. The XRD diffractograms were consisted of only two broad diffuse halo peaks. Among them, the most intense was registered between $2\theta = 20°$ and $2\theta = 35°$ and was attributed to an amorphous silicate and aluminosilicate phase consisting of SiO_4 and AlO_4 tetrahedra-sharing oxygen atoms and lacking any long-range order [14–17]. The second broad diffuse halo peak that is observed in Fig. 2 was located in-between $2\theta = 7°$ and 12° and was clearly formed only in the case of gel in the absence of aluminum (Al/Si ratio = 0). This broad halo peak was attributed to an amorphous or nanocrystalline sodium silicate hydrate phase that was generated by precipitation during the accelerated polycondensation in sodium silicate solutions and was a minor phase not exceeding 4 wt% of produced sodium silicate gel [2]. The incorporation of aluminum in the silicate gels had as a result the elimination of this secondary halo peak which was disappeared as the Al/Si molar ratio became higher than 0.167. The XRD diagrams of the sodium hydroaluminosilicates (Fig. 2) did not reveal the presence of crystalline sodium hydroxide. Therefore, it was concluded that sodium cations were consumed as network modifying agents in the formation of hydroaluminosilicates [2] and additionally as charge balancing agents for the negative charge accumulated in the areas where aluminum occurs in IV-fold coordination [1].

The heterogeneous character of the amorphous sodium hydroaluminosilicates was confirmed with scanning electron microscopy. The amorphous sodium hydroaluminosilicates were consisted of two discrete phases: (a) a gelatinous one

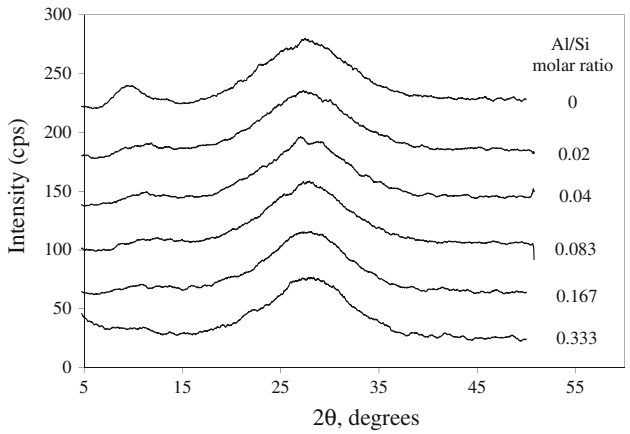

Fig. 2 XRD patterns of sodium hydroaluminosilicates with fixed SiO_2/Na_2O molar ratio 3.48 as a function of Al/Si ratio

with indefinable grain size as well as grain boundaries which was observed in all sodium hydroaluminosilicates as is seen in Fig. 3a, b, d, f, g and (b) a polymeric one with definite grains which was clearly observed in all sodium hydroaluminosilicates with Al/Si molar ratio higher than 0.04 as is seen in Fig. 3c, e, f–h. The hydroaluminosilicate with 0.02 Al/Si molar ratio (Fig. 3a) was almost exclusively gelatinous. It contained also a very small amount of inclusions as a secondary precipitation phase. As the Al/Si ratio increased, the gelatinous phase was accompanied by a polymeric one which was entrapped in the form of inclusions or deposited on the gelatinous one as is clearly seen in Fig. 3c, e–g. The polymeric phase with 0.04 Al/Si molar ratio composed of almost spherical particulates with size in-between 300 and 600 nm (Fig. 3c which is a magnification of b) which seems to have been formed by co-precipitation of silicon and aluminum in parallel and after the end of gelation. EDS analysis (Table 2) showed that the polymeric particulates were of a sodium aluminosilicate nature with Al/Si molar ratio higher than the one of the sodium aluminosilicate gels. The size of polymeric particulates increased as the Al/Si ratio was increased. The particulates in case of 0.083 Al/Si molar ratio were agglomerated and had a size in-between 600 nm and 1 μm (Fig. 3e which is a magnification of d), while at higher ratios the agglomeration was more intense forming particulates with size as big as 20 μm (Fig. 3f–h). As is mentioned above, when the Al/Si molar ratio is low (0.04–0.083) the polymeric particulates have the form of inclusions in gels, meaning that gelation and secondary precipitation took place almost simultaneously. When the Al/Si molar ratio is high (0.167–0.333), two forms of the polymeric particulates were observed; the inclusions with size in-between 300 and 800 nm (Fig. 3f, g) and the depositions on gel surface, which seem to have been formed after the end of gelation (Fig. 3f–h). The particulates in any form (inclusions or depositions) did not follow a structure pattern and therefore, they are X-rays indifferent materials. As a conclusion, the formation of the sodium aluminosilicate amorphous phases during polycondensation in sodium aluminosilicate solutions followed two different mechanisms. The gelatinous one was formed first by gelation followed by the polymeric one that was precipitated at the last stage of gelation. When the initial Al/Si molar ratio in the aqueous aluminosilicate phase was low (case of Al/Si = 0.02), gelation was almost the only process. Higher initial Al/Si ratios resulted to high supersaturation after the first stages of gelation, initiating the precipitation process. The higher the initial Al/Si ratio, the more intense the precipitation process was.

As is mentioned above, the EDS analysis in all the samples (where it was possible) showed that aluminum was preferably concentrated in polymeric phases instead of gelatinous ones as the Al/Si ratio in polymeric phases was always higher than the one in gelatinous phases. In addition, the Al/Si ratio in polymeric phases was always higher than the one of the initial aqueous sodium aluminosilicate solution from which the polymeric phases were produced (Table 2). In contrast, the Al/Si ratio in gelatinous phases was always lower than the one of the initial aqueous sodium aluminosilicate solution (Table 2). Based on the above observations and the results shown in Fig. 1, it was concluded that the hydrolytic stability of polymeric phases is substantially higher than the one of the gelatinous phases, explaining with this way the different solubility behavior of Si and Al shown in Fig. 1.

The FTIR spectrum of the amorphous sodium hydroaluminosilicates is divided in three ranges: (a) 370–1300 cm^{-1} related to the vibrational modes of –Si–O–Si– and –Si–O–Al– units, (b) 1300–1550 cm^{-1} related to the vibrational modes of carbonates, and (c) 1600–4000 cm^{-1} related to the vibrational modes of adsorbed water. The FTIR spectra in the range 370–1300 cm^{-1} at different Al/Si ratios are shown in Fig. 4a.

There are three main bands associated with different vibrations in the –Si–O–M– units (M = Al, Si) [6, 18, 19]: (a) 1000–1100 cm^{-1} due to asymmetric stretching (band I), (b) 750–800 cm^{-1} due to symmetric stretching (band II), and (c) ≈450 cm^{-1} due to bending (band III). All the observed bands in Fig. 4a were very broad absorption bands indicating the structural disorder and thus the amorphous character of the sodium hydroaluminosilicates. Band I, which is the main IR absorption band, was very broad extending in the range 850–1200 cm^{-1}. The broadness of this band is related to the wide distribution of SiQ^n structural units (where n denotes the number of bridging oxygen atoms in the first coordination sphere of Si atom) in the amorphous sodium hydroaluminosilicates [2]. The SiQ^n structural units are IR active in the range 850–1200 cm^{-1} [20, 21]. Particularly, the SiQ^4 unit is IR active around 1200 cm^{-1}, the SiQ^3 around 1100 cm^{-1}, the SiQ^2 around 950 cm^{-1}, the SiQ^1 around 900 cm^{-1}, and the SiQ^0 around

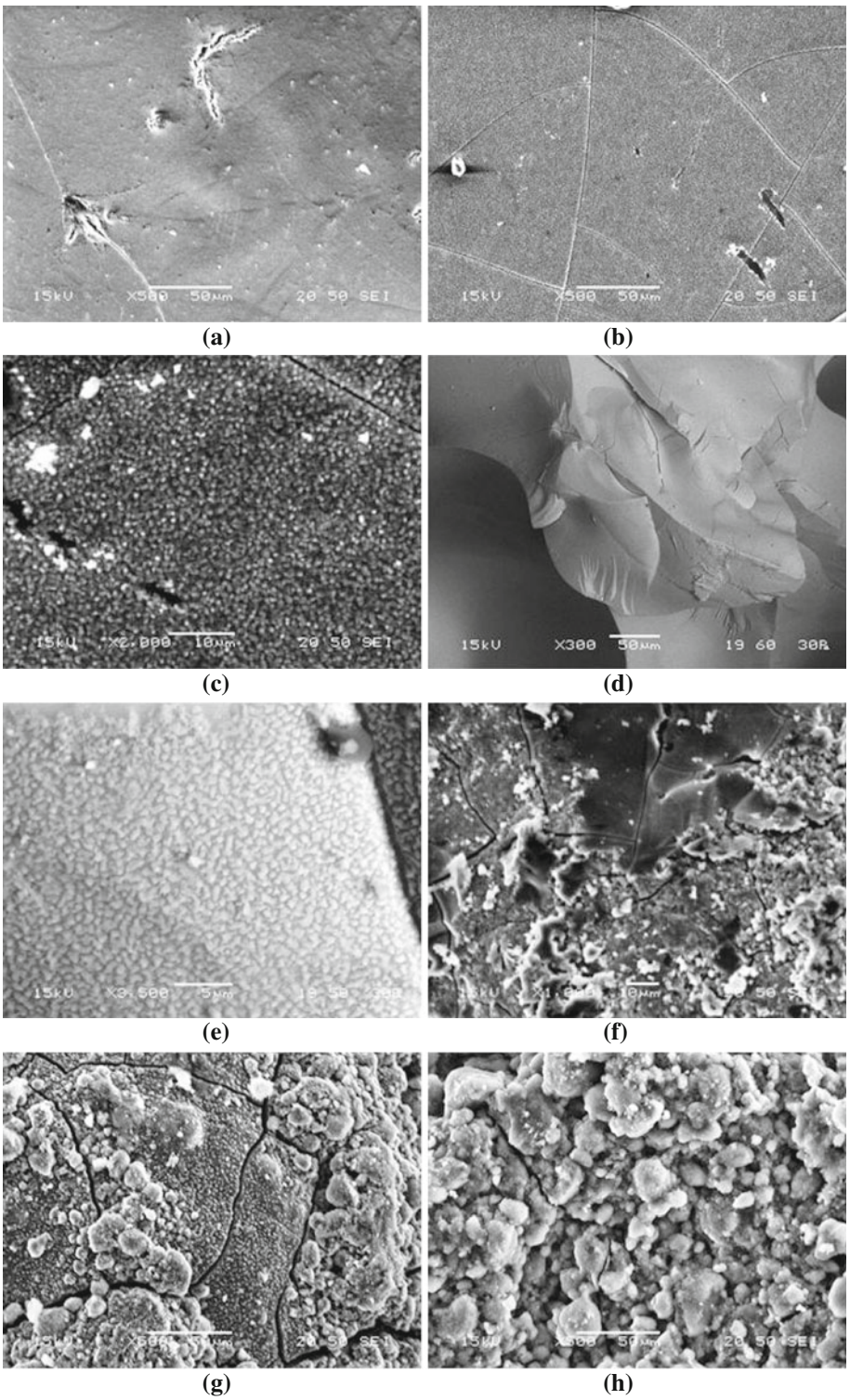

Fig. 3 SEM micrographs of sodium hydroaluminosilicates with fixed SiO_2/Na_2O molar ratio 3.48 and various Al/Si molar ratios [photos **a**–**e** were taken from fractured surfaces, while **f**–**h** from as-prepared surfaces]. **a** Al/Si = 0.02, **b** Al/Si = 0.04, **c** Al/Si = 0.04, **d** Al/Si = 0.083, **e** Al/Si = 0.083, **f** Al/Si = 0.167, **g** Al/Si = 0.333, **h** Al/Si = 0.333

850 cm^{-1}. Therefore, the broad IR spectra in the range 850–1200 cm^{-1} were the result of the overlapping of the five individual absorption bands of the SiQ^n structural units. The IR spectra showed a maximum absorption band in the range 1020–1030 cm^{-1} which is consistent with the predominance of SiQ^2 and SiQ^3 structural units over SiQ^0, SiQ^1, and SiQ^4 ones. Moreover, the maximum absorption of band I shifted systematically toward higher wavenumbers, as the Al/Si ratio increased (Fig. 4b). This shift was interpreted as an indication that the Al incorporation in silicate gels improves the cross linking in-between silicate chains and favors the structural change from SiQ^2 to SiQ^3 units

Table 2 % Atomic composition of gelatinous and polymeric phases

Initial material	Type of phase	# Sample[a]	% Si	% Al	% Na	Molar Si/Al calculated
Molar Al/Si = 0.08	Gelatinous	1	26.89	1.7	15.4	0.063
		2	25.73	1.93	14.81	0.075
		3	26.05	1.84	15.01	0.071
	Polymeric	1	24.86	2.51	14.28	0.101
		2	25.7	2.75	14.65	0.107
		3	24.42	2.38	13.94	0.097
Molar Al/Si = 0.17	Gelatinous	1	24.38	2.78	13.98	0.114
		2	24.9	3.27	14.42	0.131
		3	22.14	3.46	12.63	0.156
	Polymeric	1	23.8	4.65	13.32	0.195
		2	24.21	4.85	14.16	0.20
		3	23.03	4.51	13.1	0.196
Molar Al/Si = 0.33	Gelatinous	1	21.93	6.5	11.97	0.296
		2	21.45	6.63	12.71	0.309
		3	22.2	6.7	13.1	0.302
	Polymeric	1	19.01	7.33	10.43	0.386
		2	20.65	7.59	11.72	0.368
		3	20.4	8.76	11.25	0.429

[a] Photomicrographs are not shown in text

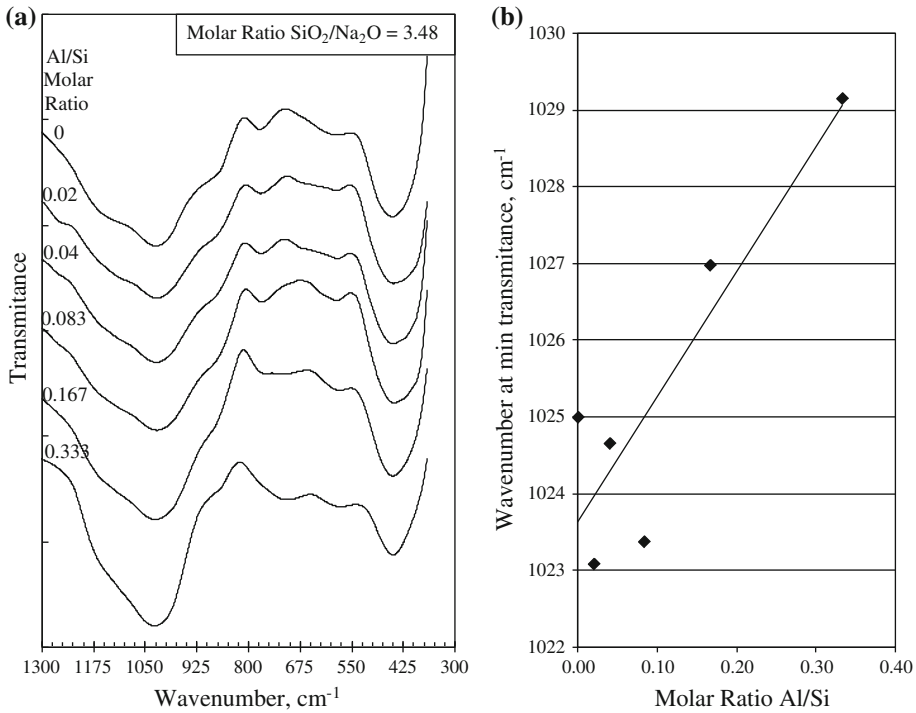

Fig. 4 **a** FTIR spectra of produced sodium hydroaluminosilicates at different Al/Si molar ratios in the range 370–1300 cm^{-1} (SiO_2/Na_2O molar ratio = 3.48), **b** shift of the wavenumber of the maximum absorption of band I as a function of the Al/Si molar ratio

which was more obvious at hydroaluminosilicates with the higher Al/Si molar ratios (0.167–0.333). Additionally, band II in the range 750–800 cm^{-1} was indicative of the structural changes as the Al/Si ratio increased (Fig. 4a). In silicate gels (ratio Al/Si = 0), a broad band around 775 cm^{-1} was observed, attributed to –Si–O–Si– vibrations [2]. As the Al/Si ratio was increased, this peak slightly shifted to lower wavenumbers and under very high Al/Si ratios it became a plateau (Al/Si molar ratio = 0.167) or shifted to 720 cm^{-1} (Al/Si molar ratio = 0.333), which corresponds to the vibrations of internal oxygen bridges of the –Si–O–Al– structural units [22]. The silicooxygen ring vibrational

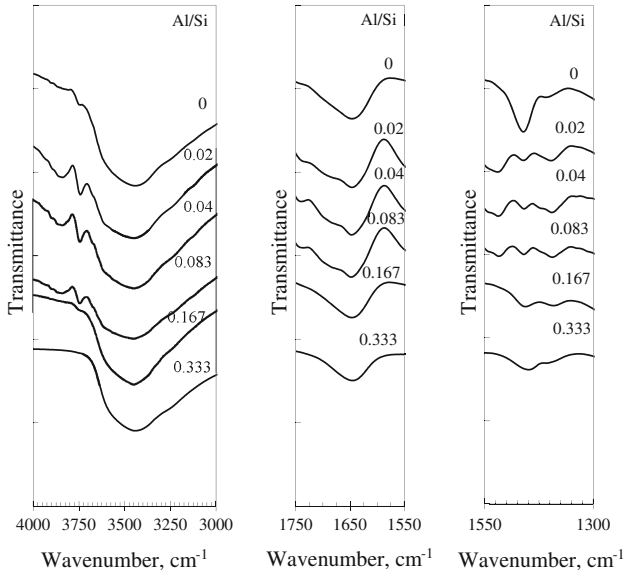

Fig. 5 FTIR spectra of produced sodium hydroaluminosilicates at different Al/Si molar ratios in the range 1300–4000 cm^{-1} (SiO_2/Na_2O molar ratio = 3.48)

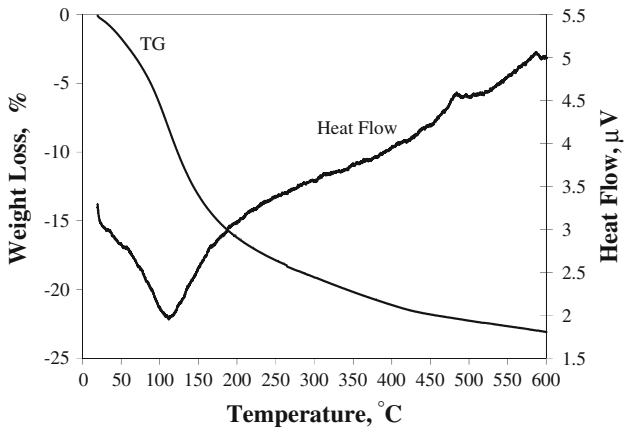

Fig. 6 TG/DTA analysis of amorphous sodium hydroaluminosilicate (Al/Si molar ratio = 0.333, SiO_2/Na_2O molar ratio = 3.48, Ar atmosphere, rate of temperature increase = 1 °C/min)

bands occurring in the wavenumber region 500–800 cm^{-1} [18, 21] were not resolved. A very weak, broad, and almost indistinct absorption band could be observed at around 600 cm^{-1} attributed to 6-membered ring vibrations, indicating that the cyclic structures in the amorphous sodium hydroaluminosilicates were almost absent.

The amorphous sodium hydroaluminosilicates prepared during the accelerated polycondensation contained water in the form of surface silanol and/or aluminol groups as well as water physically bound by hydrogen bonds to all types of surface silanol and/or aluminol groups as it was confirmed by infrared and thermogravimetric analysis. The FTIR spectra of amorphous sodium hydroaluminosilicates with different Al/Si molar ratios are shown in Fig. 5 in the range of wavenumbers 1500–4000 cm^{-1}, where the major vibrational absorption bands of water and M-OH groups (M = Al, Si) are located.

The surface silanol [23–26] and aluminol groups [27] have characteristic OH stretching vibrations in the spectra region from 3100 to 3800 cm^{-1}. The IR spectra showed a very weak absorption band at around 3750 cm^{-1} assigned to isolated non-interacting surface silanol groups [23–26]. The second feature of the IR spectra shown in Fig. 5 was the broadband located in the range of wavenumbers 3400–3700 cm^{-1}, where the absorption bands of (a) internal adjacent hydrogen bonded silanol groups (3640–3660 cm^{-1}), (b) surface vicinal hydrogen bonded silanol groups (3530–3550 cm^{-1}), and (c) several vibrational modes of surface aluminol groups (3475–3788 cm^{-1}) occur [23–27]. The maximum absorption of this broadband was centered in the region 3400–3460 cm^{-1}, which was located outside the region where the above-mentioned silanol and aluminol groups exhibit their absorption bands. This observation proved the presence of another IR active group in this region that predominated over the silanol and aluminol groups in the amorphous sodium hydroaluminosilicates. The vibrations of surface hydroxyl groups hydrogen-bonded to adsorbed water have absorption bands in the region 3400–3460 cm^{-1}, while the adsorbed water has vibrational spectra below 3300 cm^{-1} as well as around 1630 cm^{-1} [24, 26, 27]. Although the former band could not be resolved due to interferences in the broadband in-between 3400 and 3700 cm^{-1}, the latter was resolved in the IR spectra of all sodium hydroaluminosilicates shown in Fig. 5, proving the presence of surface adsorbed water molecules. The above conclusions were in accordance with the results of the thermal analysis (TG/DTA). Typical TG/DTA curves are shown in Fig. 6.

The weight loss was attributed to two different types of incorporated water in the amorphous sodium hydroaluminosilicates. The strong endothermic water removal at around 115 °C that was completed at about 200 °C was attributed to the physically adsorbed water on silanol and aluminol groups [2, 23, 24, 27]. At temperatures higher than 200 °C dehydroxylation by condensation of surface hydroxyl groups from the internal and vicinal hydrogen-bonded silanol groups took place [2, 23–25] accompanied by dehydroxylation of single (isolated) silanol as well as silanediol (geminal) groups at temperatures higher than 500 °C [23].

The amorphous sodium hydroaluminosilicates prepared by accelerated polycondensation from aluminum-containing silicate solutions were IR active in the range of 1300–1550 cm^{-1} (Fig. 5), which is related to the vibrational modes of carbonates [6, 28]. The IR spectra showed two absorption bands at around 1462 and 1400 cm^{-1}, which are related to the antisymmetric stretching of carbonate group [29–31] and were identical with the ones observed in the IR

spectra of sodium carbonate monohydrate [31], indicating the existence of a hydrogen bond between the water molecules and the CO_3^{2-} ions [30]. The addition of Al in the silicate phases resulted in some cases (Al/Si molar ratio in 0.02–0.083 region) the appearance of a new absorption band at around 1520 cm^{-1}, which was attributed to the coordination of carbonate with aluminum in the amorphous sodium hydroaluminosilicates [32]. The most obvious observation was the elimination of the band at 1462 cm^{-1} as the Al/Si ratio increased. This band was too intense in case of silicate gels (Al/Si ratio = 0) and decreased substantially with the addition of aluminum, indicating that the carbonation of the sodium aluminosilicate phases took place in substantially lesser extent. It is known that sodium ions are network modifying agents in sodium silicate gels, affecting the number of non-bridging oxygen atoms in the first coordination sphere of silicon atoms [2]. The incorporation of aluminum in sodium silicate gels had as a result the isomorphous substitution of tetrahedral Si^{4+} with tetrahedral Al^{3+} creating an excess of negative charge around aluminum sites and thus, attracting sodium cations as charge balancing agents [1, 23]. Therefore, the addition of aluminum in silicate gels under constant SiO_2/Na_2O ratio decreased the excess of sodium cations, which were consumed not only as network modifying agents but also as negative charge balancing agents, and thus their reactivity to atmospheric CO_2 avoiding the formation of carbonates.

Conclusions

The incorporation of tetra-coordinated aluminum in sodium silicate gels improves substantially their hydrolytic stability. A sodium silicate gel with SiO_2/Na_2O molar ratio 3.48, which is totally soluble in deionized water at ambient temperature, can be transformed to an insoluble amorphous sodium hydroaluminosilicate material with the addition of tetrahedral aluminum at Al/Si molar ratios higher than 0.08.

The polycondensation in aluminum-containing sodium silicate solutions follows two different mechanisms producing two X-rays indifferent sodium hydroaluminosilicate phases: a gelatinous one with indefinable grains which is the result of gelation and a polymeric one with discernible grains which is the result of precipitation. Both the phases co-exist in all sodium hydroaluminosilicates prepared in this work. The sodium hydrosilicates prepared by polycondensation in sodium silicate solutions are almost gelatinous, containing a small amount of sodium silicate hydrate as a secondary precipitation product. The addition of tetrahedral aluminum, even in small amounts, results in the formation of a polymeric phase in addition to the gelatinous one. The Al/Si ratio is always higher in the polymeric phase than in the gelatinous one, indicating the habit of aluminum to be concentrated in the polymeric phase. The polymeric phase composed of nano- and/or submicron almost spherical grains which are agglomerated as the Al/Si ratio in the initial sodium aluminosilicate solution increases.

The FTIR analysis showed that the aluminum addition causes a shift from SiQ^2 toward SiQ^3 structural units, increasing the cross-linking in-between silicate chains. Additionally, the excess of sodium cations is eliminated as they are consumed not only as network modifying agents but also as negative charge balancing agents avoiding the substantial carbonation of sodium hydroaluminosilicates.

Finally, the results of this work are very important when they are applied in the geopolymerization technology. First, they showed the superiority of easily soluble solid amorphous aluminosilicate raw materials on the silicate ones to produce water-stable geopolymers. Secondly, they showed the high potential for the production of water-stable geopolymers with low SiO_2/Na_2O ratio in case of aluminum incorporation in gels. The latter is very important from economic point of view because it can substantially decrease the waterglass utilization especially in cases where the mechanical properties of geopolymers are not of primary importance (e.g., insulation materials, fire protection materials, etc.) and thus, overcome the disadvantages of high cost and availability of waterglass that hinder the wide application of the geopolymerization technology.

Acknowledgement The authors would like to thank the Senator Committee of Basic Research of the National Technical University of Athens, Programme "PEBE-2007", R.C. No.:65/1634 for the financial support of this study.

References

1. Davidovits J (2008) Geopolymer chemistry & applications, Chap. 2, 2nd edn. Institute Géopolymère, Saint-Quentin, p 19
2. Dimas D, Giannopoulou I, Panias D (2009) J Mater Sci 44:3719. doi:10.1007/s10853-009-3497-5
3. Vallepu R, Fernandez Jimenez AM, Terai T, Mikuni A, Palomo A, Mackenzie KJD, Ikeda K (2006) J Ceram Soc Jpn 114(7):624
4. Feng D, Mikuni A, Hirano Y, Komatsu R, Ikeda K (2006) J Ceram Soc Jpn 113(1):82
5. Davidovits J (2005) Geopolymer 2005 world congress, Saint-Quentin, France, pp 9–39
6. Panias D, Giannopoulou I, Perraki T (2007) Colloids Surf A 301:246
7. Maragos I, Giannopoulou I, Panias D (2008) Miner Eng 22:196
8. Dimas D, Giannopoulou I, Panias D (2009) Miner Process Extr Metall Rev 30:211
9. Xu H, van Deventer JSJ (2000) Int J Miner Process 59:247
10. Palomo A, Grutzeck MW, Blanco MT (1999) Cem Concr Res 29:1323
11. Cheng TW, Chiu JP (2003) Miner Eng 16:205
12. Wu HC, Sun P (2007) Constr Build Mater 21:211
13. Pinto AT, Vieira E (2005) Geopolymer 2005 world congress, Saint-Quentin, France, pp 173–176

14. Davidovits J (2008) Geopolymer chemistry & applications, Chap. 4, 2nd edn. Institute Géopolymère, Saint-Quentin, p 61
15. Davidovits J (1999) Geopolymer '99 2nd international conference, Saint-Quentin, France, pp 9–39
16. Warren BE, Biscoe L (1938) J Am Ceram Soc 21(2):49
17. Warren BE, Loring AD (1935) J Am Ceram Soc 18(1–12):269
18. Hadke M, Mozgawa W (1993) Vib Spectrosc 5:75
19. Komnitsas K, Zaharaki D, Perdikatsis V (2009) J Hazard Mater 161:760
20. Clayden NJ, Esposito S, Aronne A, Pernice P (1999) J Non-Cryst Solids 258:11
21. Lecomte I, Henrist C, Liegeois M, Maseri F, Rulmont A, Cloots R (2006) J Eur Ceram Soc 26:3789
22. Mozgawa W (2001) J Mol Struct 596:129
23. Florke OW et al (2008) Silica, Ullmann's encyclopedia of industrial chemistry. Wiley-VCH Verlag GmbH & Co, Weinheim
24. Iler RK (1979) The chemistry of silica. Wiley, New York
25. Morrow BA, McFarlan AJ (1991) Langmuir 7:1695
26. Burneau A, Barres O, Gallas JP, Lavalley JC (1990) Langmuir 6:1364
27. Ranea AV, Carmichael I, Schneider FW (2009) J Phys Chem C 113:2149
28. Williams Q (1995) In: Ahrens TJ (ed) Mineral physics and crystallography: a handbook of physical constants. American Geophysical Union, Washington
29. Frost LR, Dickfos JM (2008) Spectrochim Acta A 71:143
30. Avdeeva IT, Vorsina AI (1969) Ser Khim 10:2197
31. Durie AR, Milne WJ (1967) Spectrochim Acta A 23:2885
32. Kerkhof JN, White LJ, Hem LS (1977) J Pharm Sci 66:1533